Transport Properties of Stoichiometric and Nonstoichiometric GdAs Single Crystals

doi: 10.1063/1.362814

Transport properties of stoichiometric and nonstoichiometric GdAs single crystals

D. X. Li,[a] Y. Haga, H. Shida, and T. Suzuki
Department of Physics, Tohoku University, Sendai 980-77, Japan

(Received 7 August 1995; accepted for publication 21 March 1996)

A systematic investigation of the transport properties of GdAs single crystals is presented. We report on measurements of the electric resistivity, magnetoresistance and Hall effect performed on a stoichiometric and a nonstoichiometric sample at temperatures between 1.6 and 300 K in fields up to 10 T. The stoichiometric sample behaved as a well compensated semimetal that orders antiferromagnetically, while the nonstoichiometric sample showed some anomalies that could be explained qualitatively by the model of trapped magnetic polarons. © *1996 American Institute of Physics.* [S0021-8979(96)03113-1]

I. INTRODUCTION

The rare-earth monopnictides RX (R is a rare-earth cation and X=N, P, As, Sb, and Bi) are typical strongly correlated electron systems with a low carrier concentration. Nearly all these compounds are semimetals and have the cubic rocksalt structure. In the rare-earth monopnictides, the conduction band is formed by the $5d$ orbitals of the cation R and has its minimum at the X point of the Brilloun zone, while the valence band formed mainly by the anionic np state of X (n=2, 3, 4, 5, and 6 for X=N, P, As, Sb, and Bi, respectively) has its maximum at the center of the Brilloun zone. The valencies of anion and cation cancel out, so that one could expect these materials to be semiconductors, but a weak overlap between the bottom of the conduction band and the top of the valence band is sufficient to make semimetals with a low carrier concentration out of these materials.[1,2] In the various RX compounds, the Rudermann–Kittel–Kasuya–Yosida (RKKY) exchange interaction leads to different magnetic properties, depending on the free carrier concentration. In some cases, the RKKY exchange interaction favors the ferromagnetic order, in other cases it favors the antiferromagnetic order or the spin-glass behavior. Furthermore, the strengths of the p-f mixing (between the p states of the pnictogen and the $4f$ states of the rare earth) and the d-f mixing (between the conduction $5d$ state and the $4f$ state) are different among the RX systems, due to the different energy separation between the Fermi level and the $4f$ state. Therefore it is not surprising that a variety of physical properties such as the dense Kondo effect,[3–5] the heavy fermion state,[6,7] magnetic exchange interactions,[8–10] anomalous crystalline-electric field (CEF) effect,[11,12] and the magnetic polaron effect[13–15] have been observed in RX systems. In addition, the electronic and crystalline structures of these materials are simple and permit a detailed theoretical treatment. In particular, the Ce and the Yb monopnictides, complementary for what concerns the $4f$ state, have extensively been studied experimentally[16–18] and theoretically.[4,14,19–21] Some of the anomalous properties of the Ce and Yb monopnictides could recently be explained by Kasuya *et al.*,[4,14,19–21] but there are still many unsolved problems in RX systems. With exceptions made for the Ce and Yb monopnictides, only few experiments on the magnetic and the transport properties of the other rare-earth monopnictides were performed. For the Gd monopnictides, in particular for GdAs, almost no measurement of the transport properties has been reported until now due to the difficulty of producing high quality single crystals. In order to grasp the anomalous transport properties in RX systems, further experimental studies must be performed on these compounds.

In this work, we focus our attention on the Gd monopnictides, more specifically on GdAs. GdAs is a simple magnetic reference system for the study of the magnetic exchange interactions in the rare-earth monopnictides. Gd is located in the center of the series of the rare earths in the periodic table of the elements. Therefore, the Gd^{3+} ion appearing in GdAs has a $4f^7$ configuration, which has spin 7/2 and no orbital momentum. The effects of the CEF are considered to be fairly weak in GdAs and the magnetic exchange interaction between the $4f$ spins (called f-f exchange interactions) is the main mechanism responsible for the magnetic properties of GdAs. Therefore, GdAs is a ''model'' material for the study of exchange interactions in rare-earth compounds. But the direct $4f$-$4f$ overlap between nearest-neighbor sites is weak in the rare-earth compounds, because $4f$ electrons are well screened by $5s$ and $5p$ closed shells. In GdAs (and other GdX), these f-f exchange interactions are considered to work indirectly through the d-f exchange interaction that polarizes the spins of the conduction electrons.[22] As a consequence, the electrical transport properties of GdAs appear to be strongly influenced by the magnetic states. Thus, some new physical properties, different from those observed in the Ce and Yb monopnictides, are expected for GdAs. In particular, since GdAs is an ''exchange dominating'' system with a low carrier concentration, the so-called trapped magnetic polarons can be formed and affect the transport properties.[23] However, to grow high quality single crystals of GdAs is very difficult, due to the high weld point and high vapor pressure. But recently we succeeded in growing the first large single crystals of GdAs. We reported on the magnetic properties in the preceding article.[24] In this article, we present the transport measure-

[a]Corresponding author; Present address: The Oarai Branch, Institute for Materials Research Tohoku University, Oarai, Ibaraki-ken 311-13, Japan; Electronic mail: li@jupiter.ob.imr.tohoku.ac.jp

 0021-8979/96/80(1)/264/7/$10.00

ments performed on two GdAs single crystals, a nonstoichiometric sample (GdAs No. 1) and a stoichiometric sample (GdAs No. 2).

II. EXPERIMENTAL METHODS

The two GdAs single crystals, GdAs No. 1 and GdAs No. 2, were grown by mineralization in tungsten crucibles as has been described in the preceding article.[24] In the prereaction, the components were mixed in the required amount and the initial material was synthesized in closed quartz tubes at 550 °C for six weeks. The polycrystalline materials of GdAs No. 1 and GdAs No. 2 obtained by the prereaction are pressed into hard pellets at 720 °C and 1300 atm using a glass capsule method. The hard pellets are then sealed in cleared tungsten crucibles using an electron-beam gun in vacuum. Finally, the crucibles are slowly heated to above 2500 °C, using a high-frequency induction furnace and kept at this temperature for 72 h. In this way, we obtained single crystals of $8\times6\times6$ mm^3 for GdAs No. 1 and $5\times5\times5$ mm^3 for GdAs No. 2. For both samples, x-ray diffraction patterns showed a single phase with NaCl structure. At room temperature, we determined the values of 5.895(1) Å for GdAs No. 1 and 5.864(1) Å for GdAs No. 2 for the lattice parameter. Chemical analysis yielded the values of $1:0.95\pm0.01$ and $1:1.00\pm0.01$ for the atomic ratios between Gd and As for GdAs No. 1 and GdAs No. 2, respectively. From this last analysis we concluded that GdAs No. 1 is nonstoichiometric, whereas GdAs No. 2 is stoichiometric.

The samples used for the resistivity and Hall effect experiments were cleaved from the large single crystals. The resistivity was measured by the standard four-probe method. Instead, for the Hall measurements, a four-contact geometry was used with the two voltage contacts perpendicular to the current. The samples were placed in the center of a superconducting magnet that enabled fields up to 10 T.

III. EXPERIMENTAL RESULTS

A. Electrical resistivity

The electrical resistivity $\rho(T)$ has been measured between 1.6 and 300 K for the stoichiometric and the nonstoichiometric GdAs samples, as shown in Fig. 1. The two curves are qualitatively similar. At lower temperatures, the resistivity of both samples first increases rapidly with increasing temperature, and shows a kink at the Néel temperature T_N. At higher temperatures, the resistivity becomes linear in the temperature. The Néel temperatures T_N, as determined from the derivative $\partial\rho/\partial T$, were found to be 17.2 K for GdAs No. 1 and 18.7 K for GdAs No. 2, in good agreement with our magnetic susceptibility and specific heat data.[24] The main differences between GdAs No. 1 and GdAs No. 2 consists in the residual resistivity, much larger in the nonstoichiometric sample, and in the linear slope observed in the paramagnetic phase. At $T=1.6$ K, the lowest temperature of these measurements, a residual resistivity of 5.7 $\mu\Omega$ cm was found for GdAs No. 2. In GdAs No. 1, however, the corresponding value is 55 $\mu\Omega$ cm, ten times larger than the value found for GdAs No. 2. Furthermore, the metal-like linear $\rho(T)$ behavior appears above 70 K for the stoichiometric sample, while it appears at much higher temperatures, above 200 K, for the nonstoichiometric sample.

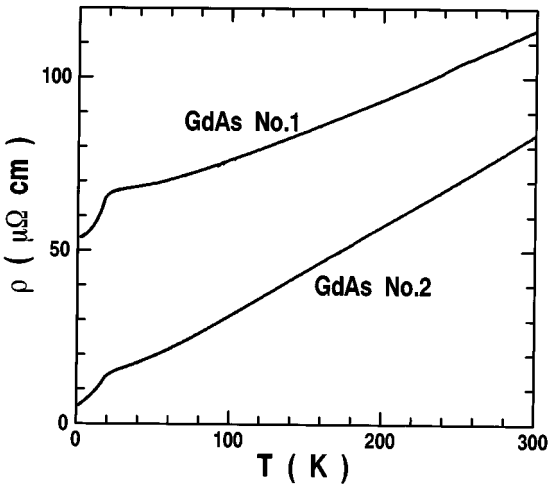

FIG. 1. Temperature dependence of the electrical resistivity for nonstoichiometric GdAs No. 1 and stoichiometric GdAs No. 2 measured at zero field.

B. Magnetoresistance

Temperature and field dependeces of the magnetoresistance were measured in the transverse configuration with the current $\mathbf{I}\|[100]$ and the field $\mathbf{H}\|[010]$. For the stoichiometric sample, the transverse magnetoresistance measured at 1.6 K (Fig. 2) follows a $\rho(H)\propto H^2$ law, and a large positive ratio $[\rho(H)-\rho(0)]/\rho(0)$ of about 8 is observed at 10 T (inset of Fig. 2). This indicates that the stoichiometric sample is a semimetallic crystal of high quality single.

The nonstoichiometric sample, however, shows an anomalous magnetoresistivity (Fig. 3). As a function of field, we established four different regimes occurring at 1.6 K, as well as at 4.2 K. In the first region ($0\ \text{T}<H<0.5$ T), ρ decreases very rapidly with increasing H. The decrease becomes even more pronounced at lower temperatures. Note

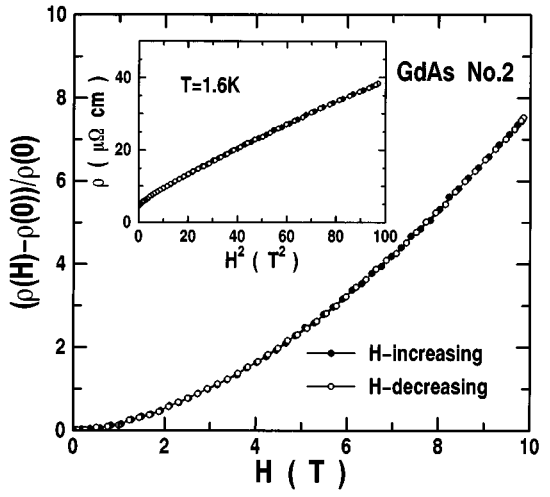

FIG. 2. Magnetic field dependence of the transverse magnetoresistance of GdAs No. 2 measured at $T=1.6$ K.

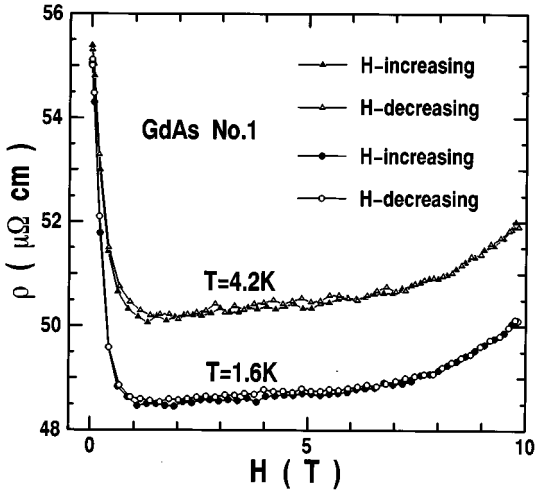

FIG. 3. Magnetic field dependence of the transverse magnetoresistance of GdAs No. 1 measured at $T=1.6$ and 4.2 K.

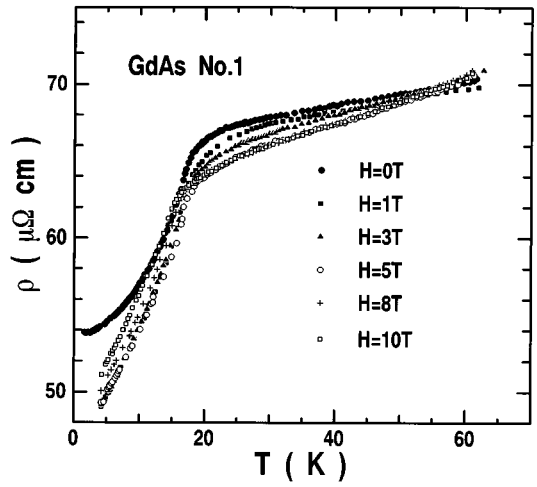

FIG. 5. Temperature dependence of the resistivity of GdAs No. 1 measured at various magnetic fields.

that the corresponding magnetization of GdAs No. 1 shows a strong increase with increasing field.[24] In the second region ($0.5\ \mathrm{T}<H<1\ \mathrm{T}$), although the magnetoresistance remains negative, the slope $|\partial\rho/\partial H|$ is considerably smaller than in the first region. Correspondingly, the increase of magnetization becomes weaker than below 0.5 T.[24] The third region ($1\ \mathrm{T}<H<7\ \mathrm{T}$) corresponds to the phase with canted spin configuration. Although the magnetoresistance becomes positive above 1 T, the slope $\partial\rho/\partial H$ is small and almost independent on field. The resistivity reaches a shallow minimum around 1 T. In the fourth region ($H>7$ T), still in the range of the canted spin configuration, the increase in ρ becomes more pronounced.

Figure 4 shows the temperature dependence of the resistivity measured on the stoichiometric sample in zero field and at 5 T. Although the magnetoresistance is positive up to 80 K, the slope $\partial\rho/\partial H$ decreases as T increases. For GdAs No. 1, a more complex temperature dependence of the magnetoresistance was observed, as shown in Fig. 5. At temperatures below T_N, $\rho(H,T)$ shows similar behavior to that illustrated in Fig. 3, i.e., the slope $\partial\rho/\partial H$ changes from negative below 1 T to positive above 1 T, but the value of $|\partial\rho/\partial H|$ becomes smaller as T increases. At $T>T_N$, the magnetoresistance remains negative up to 5 T and $|\partial\rho/\partial H|$ decreases with T, and above 5 T, $\rho(H,T)$ is becomes field independent.

C. Hall effect

The temperature and field dependences of the Hall effect were measured with $\mathbf{I}\|[100]$ and $\mathbf{H}\|[010]$. As shown in Fig. 6, at 4.2 K the Hall coefficients are field independent and negative for both samples. For the stoichiometric sample we found $R_H=-0.8\times10^{-8}\ \mathrm{m^3\,C^{-1}}$ and for the nonstoichiometric sample we found $R_H=-1.2\times10^{-8}\ \mathrm{m^3\,C^{-1}}$.

The temperature dependence of the Hall coefficients measured at $H=5$ T between 4.2 and 100 K is plotted in Fig. 7. For GdAs No. 2, R_H is negative in the measured tempera-

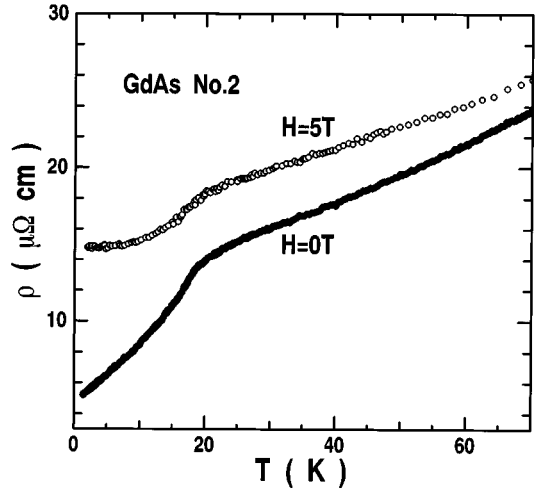

FIG. 4. Temperature dependence of the resistivity of GdAs No. 2 measured at magnetic fields of 0 and 5 T.

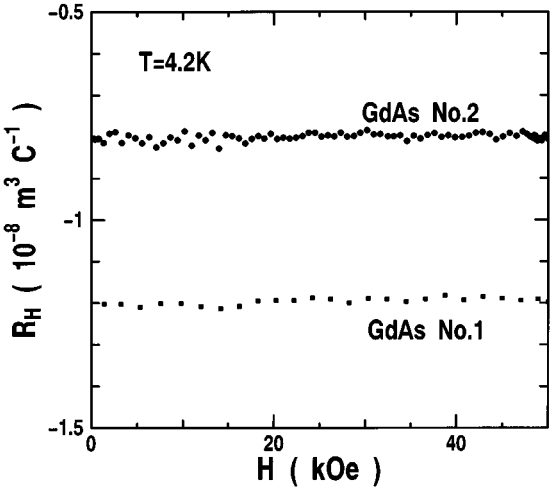

FIG. 6. Magnetic field dependence of the Hall coefficients for GdAs No. 1 and GdAs No. 2 measured at $T=4.2$ K.

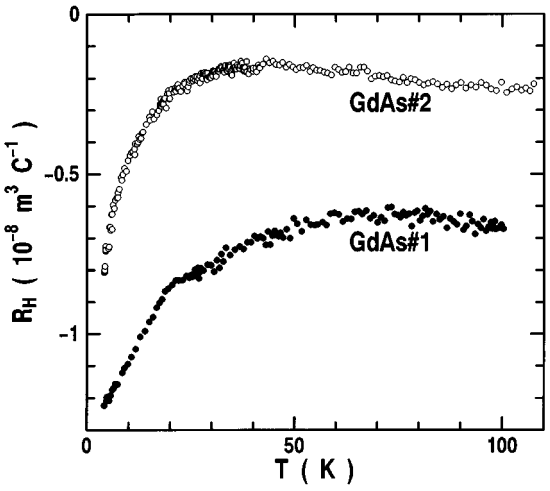

FIG. 7. Temperature dependence of the Hall coefficients for GdAs No. 1 and GdAs No. 2 measured at $H=5$ T.

ture range. Below T_N, $|R_H|$ decreases drastically with increasing T, whereas above T_N, $|R_H|$ first decreases slowly then goes through a broad minimum centered at about 40 K and finally increases slowly. For the nonstoichiometric GdAs No. 1, R_H is also negative in the measured temperature range and a broad maximum is observed in the paramagnetic phase around 70 K. Compared with GdAs No. 2, however, R_H is linear below T_N and a kink appears near T_N. Above 70 K, $|R_H|$ increases very weakly. At all measured temperatures, $|R_H|$ is larger in GdAs No. 1 than in GdAs No. 2.

IV. DISCUSSION

A. Electrical resistivity

For the stoichiometric sample, the temperature dependence of the resistivity, shown in Fig. 1, has two contributions. The first one is the normal resistivity ρ_p, caused by the electron–phonon scattering, which is linear in T at high temperatures. The second contribution is the magnetic part ρ_m of the resistivity. At low temperatures, ρ_m is generally understood to be originated from the electron–magnon scattering. The formal treatment of this last scattering mechanism has been carried out by Andersen and his collaborators.[25] For $T\rightarrow 0$, there are no magnon and phonon excited in the crystal and both resistivities ρ_p and ρ_m vanish. In absence of any impurity, the conduction electrons propagate through the perfectly periodic lattice without being scattered incoherently and the resistivities ρ_p and ρ_m vanish. With increasing temperature, the conduction electrons are scattered off the thermally activated magnons and, in a ferromagnetic or antiferromagnetic metal, ρ_m contributes to the electrical resistivity together with the contributions of the electron–phonon and electron-impurity scattering. Spin waves (magnons) are the collective excitations of the aligned spins, just like phonons in the case of lattice vibrations. The electron–magnon scattering resistivity increases nonlinearly with increasing temperature. It may be the origin of the nonlinear increase of the resistivity observed in stoichiometric GdAs sample at low temperatures (Fig. 1).

As the temperature is increased further, more and more magnetic ions can have their spin orientations affected by thermal fluctuations. In this case, the spin-disorder scattering is usually considered to be the origin of the scattering process. In the gadolinium monopnictides, this spin-disorder scattering may be caused by the d-f coulomb exchange interaction, i.e., the RKKY exchange interaction, in which the conduction $5d$ electrons interact with the f electrons, considered to be well localized.[22] Above T_N, the spins of the magnetic ions become randomly oriented and the magnetic part of the resistivity, originated from the scattering between the conduction electrons and the spin disorder, saturates and becomes independent of temperature. Kasuya[26] calculated the contribution to the magnetic part of the electrical resistivity originated from this d-f scattering process for magnetic metals with magnetic ions in the S state (quenched orbital moment). Above the Néel temperature, this calculation yields a magnetic resistivity inversely proportional to the carrier concentration. We have measured the values of $\Delta\rho=\rho(T=T_N)-\rho(T\rightarrow 0)$ for all single crystals of GdX (X =P, As, Sb, and Bi), and observed that $\Delta\rho$ decreases when going from GdP to GdBi. For GdAs, the value of $\Delta\rho$ is about twice the value found for GdSb. This is in accord with Kasuya's theory, since our de Haas–van Alphen (dHvA) effect measurements show that the carrier concentration in GdSb is about double as in GdAs. Thus, in stoichiometric GdAs, the magnetic resistivity is considered to originate from the RKKY interaction between the conduction $5d$ electrons and the $4f$ electrons. But the critical scattering due to the short-range order is also important and affects the resistivity near the Néel temperature.[27] The fact that the warping of the $\rho(T)\sim T$ curve begins at a temperature slightly above the Néel point may be attributed to the critical scattering process. This is also applicable to the nonstoichiometric GdAs sample. The electron–phonon scattering contribution to the resistivity, linear in T, dominates the measured resistivity of the stoichiometric GdAs sample above 70 K, while in the nonstoichiometric sample the resistivity is nonlinear up to 200 K. Because the Néel temperatures are nearly the same in both GdAs No. 1 and GdAs No. 2, and the critical scattering is important only near the Néel temperature, it is natural to believe that the critical scattering vanishes near 70 K in GdAs No. 1, as it does in GdAs No. 2, when the resistivity observed for the stoichiometric sample becomes linear in temperature. The origin of the nonlinear resistivity between 70 and 200 K in the nonstoichiometric GdAs sample is therefore thought to be not only due to the critical scattering, but also due to another additional scattering process, considered to find its origin in the formation of trapped magnetic polarons.

The formation of the trapped magnetic polarons in nonstoichiometric GdAs has already been described in a recent short communication.[15] The basic idea is the following. In considering the state of a conduction electron in an antiferromagnetic crystal, it is customary to assume that it does not disturb the magnetic ordering of the crystal. In some cases, however (for example, in low carrier systems), an energetically more favorable state is achieved when the electrons become localized and interact with the surrounding magnetic

ions.[28] In the nonstoichiometric GdAs sample, some electrons, originated from the As vacancies, are trapped by the coulomb potential of the As vacancies. The strong d-f exchange interaction between the trapped electrons and the neighboring $4f$ spins aligns the $4f$ spins. A trapped electron generates a region with ferromagnetic ordered $4f$ spins around itself and a trapped magnetic polaron (TMP) is formed. When the As vacancies move through the crystal, the trapped magnetic polarons automatically also move.

For the conduction electrons, the formation of trapped magnetic polarons in nonstoichiometric GdAs results in an additional scattering, superimposed on the intrinsic scattering of pure GdAs. This leads to the large residual resistivity, the large change of $d\rho/dT$ around T_N, and the nonlinear ρ-T behavior up to 200 K. This explanation is also in accord with our susceptibility measurements, from which we deduced that the trapped magnetic polaron states formed in nonstoichiometric GdAs are disintegrated above 200 K.[24]

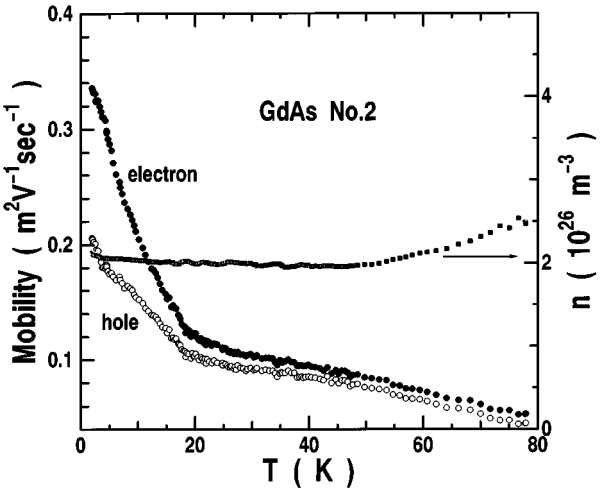

FIG. 8. Temperature dependence of the mobilities (of electron and hole) and carrier concentration calculated with two band model.

B. Magnetoresistance

Transverse magnetoresistance measurements enable to check the sample quality of a semimetal. In general, in a semimetal, the existence of lattice defects, originating from impurities or nonstoichiometry, broadens the Landau levels. When the energy interval between the Landau levels is smaller than the level broadening, then $[\rho(H)-\rho(0)]/\rho(0)<1$ and the dHvA or Schubnikov–de Haas (SdH) signals cannot be observed.[29] For a semimetallic single crystal of high quality, in general, one observes the dHvA or SdH signals, a large value for $[\rho(H)-\rho(0)]/\rho(0)$, a large value for the resistivity ratio $\rho(T=300\ \mathrm{K})/\rho(T\rightarrow 0)$ and an approximate $\rho(H)\propto H^2$ behavior. The stoichiometric GdAs No. 2 sample can be considered to be a high quality single crystal because clear dHvA signals have been observed, the transverse magnetoresistivity measured at 4.2 K shows a large ratio $[\rho(H)-\rho(0)]/\rho(0)\approx 8$ at 10 T, the residual resistivity of GdAs No. 2 is only 5.5 $\mu\Omega$ cm and, consequently, a large residual resistance ratio $\rho(T=300\ \mathrm{K})/\rho(T\rightarrow 0)$ of 16.7 is observed. Thus, the experimental results obtained for this sample represent intrinsic features of pure GdAs.

In the nonstoichiometric GdAs No. 1 sample, a large and negative magnetoresistance was observed at low temperatures and low magnetic fields. We interpret this anomaly as an indication of the formation of trapped magnetic polarons. Indeed, at zero field, the trapped magnetic polarons have randomly oriented moments, yielding a large contribution to the resistivity through the electron–polaron scattering. With increasing temperature, the d-f exchange interaction within the polarons becomes gradually weakened by thermal fluctuations. This explains why below 0.5 T $|d\rho/dH|$ is smaller at 4.2 K than at 1.6 K. Similarly, with increasing field, the moments of the polarons, canted in low fields, are rapidly aligned to the ferromagnetic configuration. As a consequence, a pronounced drop appears in the resistivity with increasing field in the low-field region. As the field is raised further, the effect of the magnetic polarons on the resistivity becomes smaller, and gradually the intrinsic positive magnetoresistance of the semimetal becomes dominant. Finally, above 7 T, the scattering off the trapped magnetic polaron mechanism is not expected, and the magnetoresistance of GdAs No. 1 approximately follows $\rho(H)\propto H^2$ law, similar to the stoichiometric GdAs No. 2 sample.

C. Hall effect

In magnetic materials, the Hall resistivity has two contributions and is often expressed as

$$\rho_H = R_0 B + R_S M, \tag{1}$$

where B is the applied magnetic field, and R_0 and R_S are referred to as the normal and the anomalous Hall coefficients, respectively. For the nonstoichiometric GdAs No. 1 sample, a constant Hall coefficient R_H was observed, although at low fields our measurements show a clearly nonlinear magnetization.[24] This means that the anomalous Hall effect is negligible compared to the normal Hall effect. Therefore, the Hall coefficient measured for GdAs is given by the normal Hall effect at all temperatures and magnetic fields (Fig. 6). It appears to be usual that, in low carrier systems, the normal Hall effect generally dominates the measured Hall signal.

The stoichiometric GdAs No. 2 sample is considered to be a well compensated semimetal. Therefore, three parameters are necessary to reproduce the electrical transport measurements. These are the concentration of conduction electrons and valence holes ($n=n_e=n_h$) and the mobilities (μ_e,μ_h) of the conduction electrons and the valence holes. Neglecting the anomalous Hall effect and the field dependence of the mobilities and carrier concentrations,[30] the electrical resistivity, Hall constant, and transverse magnetoresistance are determined in a two band model as follows:[31]

$$1/\rho(0,T) = ne(\mu_h+\mu_e), \tag{2}$$

$$R_H(H,T) = (\mu_h-\mu_e)/[ne(\mu_h+\mu_e)], \tag{3}$$

$$[\rho(H,T)-\rho(0,T)]/\rho(0,T) = \mu_h\mu_e H^2. \tag{4}$$

From Eqs. (2)–(4), we can determine the three parameters (n, μ_e, and μ_h). In Fig. 8 we show the resulting temperature

dependence of the parameters n, μ_e, and μ_h for GdAs No. 2. At 4.2 K, we find a free carrier concentration of $n=2.07\times10^{20}$ cm^{-3}=0.010(4) per Gd atom. Recently, we could observe clear dHvA signals for GdAs No. 2. The carrier number determined from the dHvA effect measurements is 0.011 per Gd atom which is consistent with the Hall effect measurements. The mobility of the electrons is larger than that of the holes in the investigated temperature range. This explains the measured negative Hall coefficient. Around T_N, both mobilities μ_e and μ_h show an abrupt change in agreement with the above given analysis of the magnetic scattering around T_N. Below T_N, the difference between μ_e and μ_h rapidly increases with decreasing T, while the carrier concentration n slowly increases. According to Eq. (3), the increase of n will cause a decrease of $|R_H|$, but the experiments (Fig. 7) have shown that $|R_H|$ still increases at low temperatures. Thus, the rapid increase of $|R_H|$ below T_N seems to be determined by an increase in the mobilities. Furthermore, the slopes of all three curves of μ_e, μ_h, and n (Fig. 8) vary slightly near 45 K. This may be related to the broad maximum of R_H that has appeared around the same temperature. The origin of the relatively rapid increase of n and decrease of μ_e and μ_h at $T>45$ K is not known yet.

The temperature dependences of the mobilities shown in Fig. 8 could also be discussed in the same context as the phenomenological interpretation of the resistivity data described above. The rapid increase of the mobilities below T_N originates from the rapid decrease of magnetic scattering and leads to the rapid decrease of the resistivity. Above and near T_N, the mobilities are affected by the electron–phonon scattering and the critical scattering. At $T\gg T_N$, the decrease of the mobilities is mainly stem from the increasing electron–phonon scattering, which leads to the observed increase of resistivity with increasing T.

It is interesting to notice that, using Eqs. (2)–(4), a similar calculation has been made for stoichiometric YbAs by Oyamada *et al.*[30] The results confirm that the mobility of holes in YbAs does not increase below 80 K while the mobility of electrons increases strongly. This indicates that, at low temperatures, in YbAs, the resistivity is mainly determined by the mobility of the electrons. However, our results for stoichiometric GdAs No. 2 (Fig. 8) show that the mobility of the holes clearly increases below T_N, though always being lower than the mobility of the electrons. Thus, even at low temperatures, the contribution of the holes to resistivity cannot be ignored in GdAs. Recently, we have also made a similar analysis for stoichiometric GdSb, and we obtained nearly equal mobilities of holes and electrons. However, for a different RX system, one should normally expect different electron and hole mobilities, as a consequence of the difference in the $4f$ level, the CEF splitting, and the electronic structure.

It should be emphasized that, in the above analysis, only the classical scattering and the normal Hall effect are considered. Thus, it is an approximate calculation and further studies are necessary. Equations (2)–(4) are applicable only for compensated semimetals. Therefore, the nonstoichiometric GdAs No. 1 sample does not show the above described magnetoresistance, intrinsic for a well compensated semimetal. In GdAs No. 1, the electron and hole mobilities are affected by the formation of trapped magnetic polarons. Particularly at low temperatures and low magnetic fields, the assumption of field independent mobilities is no longer valid for nonstoichiometric GdAs. The electron and hole mobilities in GdAs No. 1 are expected to increase drastically with increasing H due to the rapid decrease of the effect of the scattering off the trapped magnetic polarons. Thus, in GdAs No. 1, at low temperatures and low magnetic fields we expect smaller mobilities for electrons and holes than we observed in GdAs No. 2. With increasing field, the effect of the scattering off trapped magnetic polarons decreases rapidly. For $H>7$ T or $T>200$ K, the effect of the trapped magnetic polarons is expected to vanish and the temperature dependences of the mobilities of GdAs No. 1 are expected to become the same as those observed in GdAs No. 2.

With increasing carrier concentration, the Fermi energy increases and even overcomes the coulomb correlation energy in the limiting case of a high carrier concentration. In the latter case the trapped magnetic polarons cannot be formed. Thus, the effect of trapped magnetic polarons is important only in low carrier systems, i.e., in strongly correlated electron systems. In fact, effects of trapped magnetic polarons have been clearly found in nonstoichiometric semiconductors as EuTe[32,33] and other Eu-chalcogenides[34] with very low carrier concentrations, and some theoretical studies[35] have been carried out for these materials. For semimetals, however, the formation of trapped magnetic polarons has been observed for the first time, to the best of our knowledge, in our recent experiments. In contrast to the Eu chalcogenides, the d-f mixing can be ignored in GdX because the $4f$ level is deep and an additional RKKY interaction becomes important, as discussed in Ref. 36. The carrier concentrations in GdX are higher than 10^{20} cm^{-3} and therefore much larger than in semiconducting Eu chalcogenides ($<10^{19}$ cm^{-3}). A vacancy of a chalcogen atom in the Eu chalcogenides is a doubly charged donor, whereas a defect of a pnictogen atom in GdX is a triply charged donor. The former case has recently been investigated by Umehara[35] in a He-like model for EuTe with singlet or triplet spin configurations of the electrons doped by impurities. Such a model is not suited for the Gd monopnictides, because of the different electronic configuration. Therefore, the formation of trapped magnetic polarons in GdX presents both experimental and theoretical interests.

V. CONCLUSION

The transport properties of both stoichiometric and nonstoichiometric GdAs single crystals have been investigated by measuring their resistivity, magnetoresistance, and Hall effect. Stoichiometric GdAs behaves as expected for a well compensated semimetal. The temperature dependence of the resistivity can be explained by the d-f coulomb scattering at lower temperatures. A simple calculation yields that the observed rapid change of the Hall coefficient R_H below T_N is due to the increasing mobilities of the conduction electrons and valence holes. At 4.2 K, the carrier concentration determined from the Hall effect measurements is 0.010(4) per Gd atom, consistent with the dHvA measurements. The scatter-

ing mechanisms appearing in stoichiometric GdAs are considered to appear also in nonstoichiometric GdAs. But, compared with stoichiometric GdAs, nonstoichiometric GdAs shows some anomalies in the transport properties such as a large negative magnetoresistance and a nonlinear resistivity at higher temperatures. These anomalies can be qualitatively understood within the framework of the trapped magnetic polaron model.

ACKNOWLEDGMENTS

The authors would like to thank Dr. M. Umehara for helpful discussions and Dr. R. Pittini for help in preparing the manuscript.

[1] A. Hasegawa and A. Yanase, J. Phys. Soc. Jpn. **42**, 492 (1977).
[2] T. Kasuya, O. Sakai, J. Tanaka, H. Kitazawa, and T. Suzuki, J. Magn. Magn. Mater. **63&64**, 9 (1987).
[3] T. Kasuya, Y.S. Kwon, T. Suzuki, K. Nakanish, F. Ishigama, and K. Takegahara, J. Magn. Magn. Mater. **90**,**91**, 389 (1990).
[4] T. Kasuya, A. Oyamada, M. Sera, Y. Haga, and T. Suzuki, Phys. B **199&200**, 585 (1994).
[5] D. X. Li, A. Oyamada, H. Shida, T. Suzuki, T. Kasuya, A. Dönni, and F. Hulliger, Phys. B **186–188**, 547 (1993).
[6] T. Sakon, N. Sato, A. Oyamada, N. Takeda, T. Suzuki, and T. Komatsubara, J. Phys. Soc. Jpn. **61**, 2209 (1992).
[7] T. Kasuya, Jpn. J. Appl. Phys. **8**, 3 (1993).
[8] H. Takahashi and T. Kasuya, J. Phys. C **18**, 2697, 2709, 2721, 2731, 2745, 2755 (1985).
[9] D. X. Li, Y. Haga, H. Shida, and T. Suzuki, Phys. B **199&200**, 631 (1994).
[10] T. Kasuya, J. Alloys Compd. **192**, 217 (1993).
[11] B. R. Cooper and O. Vogt, Phys. Rev. B **1**, 1211 (1970).
[12] D. X. Li, Y. Haga, H. Shida, T. Suzuki, A. Kido, S. Nimori, and G. Kido, Phys. B **199&200**, 609 (1994).
[13] M. Kohgi, T. Osakaba, K. Kakurai, T. Suzuki, Y. Haga, and T. Kasuya, Phys. Rev. B **49**, 7068 (1994).
[14] T. Kasuya, J. Phys. Soc. Jpn. **63**, 843 (1994).
[15] D. X. Li, Y. Haga, H. Shida, A. Omino, and T. Suzuki, Solid State Commun. **93**, 319 (1995).
[16] T. Suzuki, Jpn. J. Appl. Phys. **8**, 267 (1993).
[17] T. Suzuki, Phys. B **186&188**, 347 (1993).
[18] D. X. Li, A. Oyamada, K. Hashi, Y. Haga, T. Matsumura, H. Shida, T. Suzuki, T. Kasuya, A. Dönni, and F. Hulliger, J. Magn. Magn. Mater. **140–144**, 1169 (1995).
[19] T. Kasuya, Y. Haga, Y. S. Kwon, and T. Suzuki, Phys. B **186&188**, 9 (1993).
[20] T. Kasuya and T. Suzuki, J. Phys. Soc. Jpn. **61**, 2628 (1992).
[21] T. Kasuya, T. Suzuki, and Y. Haga, J. Phys. Soc. Jpn. **62**, 2549 (1993).
[22] A. Narita and T. Kasuya, J. Magn. Magn. Mater. **52**, 373 (1985).
[23] M. Umehara, Phys. Rev. B **36**, 574 (1987).
[24] D. X. Li, Y. Haga, H. Shida, and T. Suzuki, Phys. Rev. B **53**, 8473 (1996).
[25] N. H. Andersen and H. Smith, Phys. Rev. B **19**, 384 (1979).
[26] T. Kasuya, Prog. Theor. Phys. **16**, 58 (1956).
[27] T. G. Richard and D. J. W. Geldart, Phys. Rev. B **15**, 1502 (1977).
[28] E. L. Nagaev, JETP Lett. **6**, 18 (1967).
[29] C. Kittle, in *Introduction to Solid State Physics*, sixth ed., edited by R. McConnin (Wiley, New York, 1986).
[30] A. Oyamada, C. Ayache, T. Suzuki, J. Rossat-Mignod, and T. Kasuya, J. Magn. Magn. Mater. **90&91**, 443 (1990).
[31] H. Nozaki, H. Wada, and S. Takekawa, J. Phys. Soc. Jpn. **60**, 3510 (1991).
[32] Y. Shapira, S. Foner, N. F. Oliveira, Jr., and T. B. Reed, Phys. Rev. B **5**, 2647 (1972).
[33] N. F. Oliveira, Jr., S. Foner, Y. Shapira, and T. B. Reed, Phys. Rev. B **5**, 2634 (1972).
[34] S. von Molner and S. Methfessel, J. Appl. Phys. **38**, 959 (1967).
[35] For example, M. Umehara, Phys. Rev. B **46**, 12323 (1992).
[36] P. Wachter and E. Kaldis, Solid State Commun. **34**, 241 (1980).